Mechanism of the Reaction of Cuboidal $[Mo_3FeS_4(H_2O)_{10}]^{4+}$ with Dioxygen†

Paul W. Dimmock and A. Geoffrey Sykes *

Department of Chemistry, The University, Newcastle upon Tyne NE1 7RU

Solutions of the grey-purple mixed-metal cuboidal aqua ion $[Mo_3FeS_4(H_2O)_{10}]^{4+}$ react with O_2 to give the now well characterised (green) incomplete cuboidal $[Mo_3S_4(H_2O)_9]^{4+}$ and Fe^{2+} in a two-electron (per cube) redox process. With the cube in excess, spectrophotometric changes are consistent with the stoicheiometric equation: $2Mo_3FeS_4^{4+} + O_2 + 4H^+ \longrightarrow 2Mo_3S_4^{4+} + 2Fe^{2+} + 2H_2O$. First-order rate constants $k_{obs.}$ monitored at the $[Mo_3S_4(H_2O)_9]^{4+}$ peak at 367 nm ($\Delta\varepsilon$ = 4 570 M^{-1} cm^{-1}) with $[Mo_3FeS_4(H_2O)_{10}]^{4+}$ in >10-fold excess can be expressed as $2k[Mo_3FeS_4^{4+}]$. On varying $[H^+]$, $k = a + b[H^+]$, where at 25 °C a = 0.43 M^{-1} s^{-1} and b = 0.26 M^{-2} s^{-1}, I = 2.0 M($LiClO_4$). With O_2 in large excess spectrophotometric evidence (245 nm) has been obtained for an intermediate believed to be $Mo_3FeS_4(O_2)^{4+}$, and a reaction sequence $Mo_3FeS_4^{4+} + O_2 \overset{K_1}{\rightleftharpoons} Mo_3FeS_4(O_2)^{4+}$, followed by $Mo_3FeS_4(O_2)^{4+} \xrightarrow{k_2} Mo_3S_4^{4+} + (FeO_2)$, is proposed. With $[Mo_3FeS_4(H_2O)_{10}]^{4+}$ in excess the reaction $(FeO_2) + Mo_3FeS_4^{4+} + 4H^+ \longrightarrow Mo_3S_4^{4+} + 2Fe^{2+} + 2H_2O$ occurs, but is relatively fast and k remains equal to K_1k_2. With O_2 in excess the slower Fe^{2+}/Fe^{3+}-catalysed decomposition of the peroxide released is observed, and Fe^{3+} (up to 30% of Fe) is obtained as a product. The stoicheiometry is therefore less than the 2:1 observed with $[Mo_3FeS_4(H_2O)_{10}]^{4+}$ in excess. An alternative mechanism involving formation of the adduct $[Mo_3FeS_4O_2Mo_3FeS_4]^{8+}$ does not explain these features, but may make some contribution with the reactant $[Mo_3FeS_4(H_2O)_{10}]^{4+}$ in excess.

Redox reactions of dioxygen with transition-metal complexes in solution continue to attract much attention because of their fundamental importance and relevance to chemical and biological processes.[1] Although outer-sphere oxidations have been identified,[2] in many cases the intermediates and products observed are consistent with inner-sphere processes.[3] Extensive studies on the reactions of cobalt(II) complexes with O_2 have led to the identification of 1:1 adducts formulated as $Co^{III}–O_2^-$, as well as 2:1 μ-peroxo Co^{III}_2 products of the kind CoO_2Co^{4+}.[3,4] Other studies on the reaction of O_2 with single-electron reductants such as Cr^{II},[5] Ru^{II},[2a,6] Fe^{II},[7] and Cu^{I},[8] have been carried out. In contrast less is known about reactions in which the metal undergoes a two-electron change. Two studies with the aqua ions of Mo^{III},[9] and V^{II},[10] as reductant have been reported. In keeping with the requirement that two-electron changes tend to proceed by inner-sphere processes, both these reactions proceed with the formation of inner-sphere adducts.

Shibahara *et al.*[11] have prepared the mixed-metal cuboidal complex $[Mo_3FeS_4(H_2O)_{10}]^{4+}$ by treating the incomplete cuboidal Mo^{IV}_3 ion $[Mo_3S_4(H_2O)_9]^{4+}$ with metallic Fe. From *X*-ray crystallography on the ammine complex $[Mo_3FeS_4(NH_3)_9(H_2O)]Cl_4$, the three Mo atoms retain their distorted-octahedral co-ordination, but the Fe is tetrahedral.[11] An alternative route for the preparation is the treatment of $[Mo_3S_4(H_2O)_9]^{4+}$ with Fe^{2+} in the presence of $NaBH_4$.[12] The cluster has an even number of electrons and does not give an e.p.r. spectrum.[13] From magnetic measurements (22 °C) the product is paramagnetic with two unpaired electrons.[13] These and other solution properties including Mössbauer measurements, which indicate a high-spin coupled iron(III) centre, are reported elsewhere.[13] One property of $[Mo_3FeS_4(H_2O)_{10}]^{4+}$ which is considered in this study is the sensitivity to dioxygen. Since metal atoms in the cube are metal–metal bonded, the tetrahedral Fe (co-ordinated to three μ_3-sulphido ligands and an H_2O) is in a unique situation as far as aqueous iron co-ordination chemistry is concerned.[13] With Ni the analogous complex $[Mo_3NiS_4(H_2O)_{10}]^{4+}$ has been characterised.[14] However, in the case of the odd-electron Co- and Cu-containing clusters, dimeric forms $[\{Mo_3CoS_4(H_2O)_9\}_2]^{8+}$ and $[\{Mo_3CuS_4(H_2O)_9\}_2]^{8+}$ have been identified.[15,16] No evidence has been obtained for the dimerisation of $[Mo_3FeS_4(H_2O)_{10}]^{4+}$, which conforms to Beer's law, and in kinetic studies with $[Fe(H_2O)_6]^{3+}$ and $[Co(dipic)_2]^-$ (dipic = dipicolinate = pyridine-2,6-dicarboxylate) as oxidants, the rate laws indicate reactions of the monomer cube only.[13] In this work, also at I = 2.00 M ($LiClO_4$), monomer forms are assumed to be present.

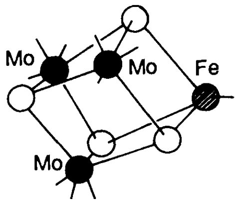

Experimental

Preparation of $[Mo_3FeS_4(H_2O)_{10}]^{4+}$.—Iron wire (1 g; Johnson Matthey, Specpure) was added to $[Mo_3S_4(H_2O)_9]^{4+}$ (50 cm^3 of 1 mM) in 2.0 M $HClO_4$,[11,13] and allowed to react for ≈1 h under rigorous O_2-free conditions (N_2 gas). Purification was by loading a solution diluted to <0.5 M $HClO_4$ onto an O_2-free Dowex 50W-X2 cation-exchange column (1 cm × 20 cm). The column was washed with 0.5 M (100 cm^3) followed by 1.0 M $HClO_4$ (100 cm^3) and then eluted with 2.0 M $HClO_4$. The grey-purple $[Mo_3FeS_4(H_2O)_{10}]^{4+}$ was eluted (<24 h before use) prior to green $[Mo_3S_4(H_2O)_9]^{4+}$. Storage at 4 °C was under N_2 in a flask, also under N_2 in a glass bottle. Relevant

---

† *Non-S.I. unit employed:* M = mol dm^{-3}.

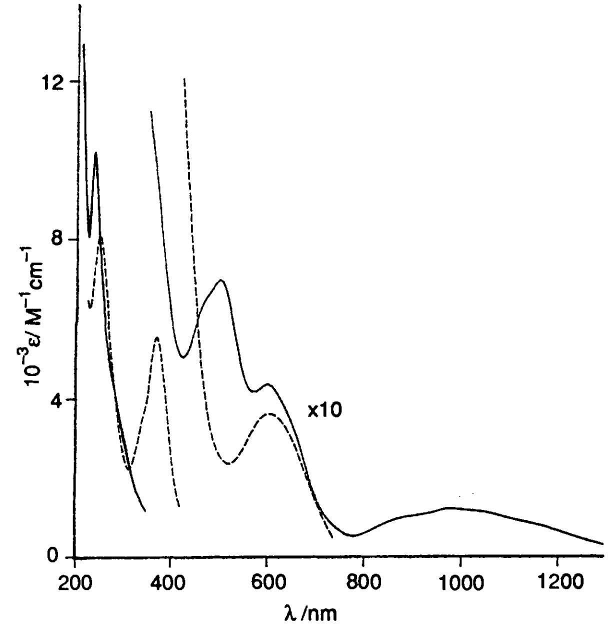

Figure 1. U.v.–visible–near-i.r. absorbance spectra of $[Mo_3FeS_4(H_2O)_{10}]^{4+}$ (——) and $[Mo_3S_4(H_2O)_9]^{4+}$ (- - - -) in 2.0 M $HClO_4$

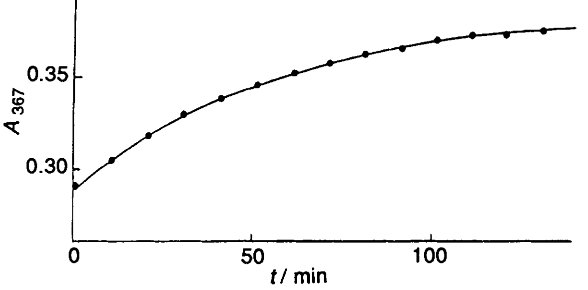

Figure 2. Absorbance changes with time for the reaction of $[Mo_3FeS_4(H_2O)_{10}]^{4+}$ (0.20 mM) with O_2 (0.01 mM) at 25 °C, I = 2.00 M ($LiClO_4$), monitored at 367 nm

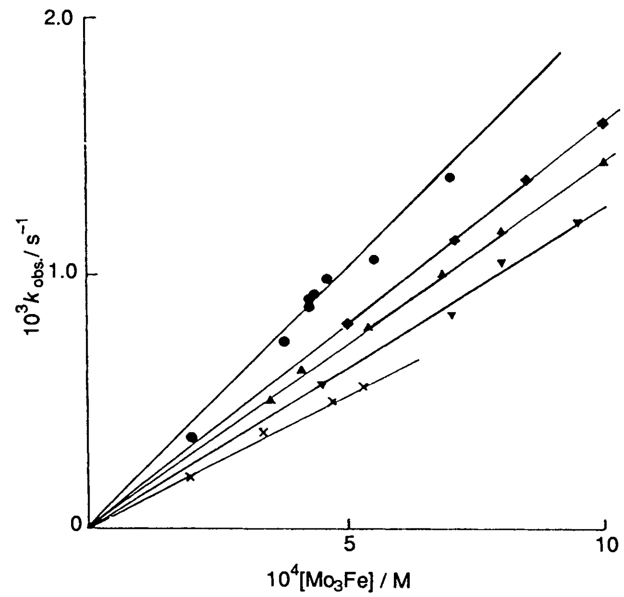

Figure 3. Dependence of first-order rate constants $k_{obs.}$ (25 °C) for the reaction of $[Mo_3FeS_4(H_2O)_{10}]^{4+}$ (reactant in > 10-fold excess) with O_2 on the concentration of $[Mo_3FeS_4(H_2O)_{10}]^{4+}$, I = 2.00 M ($LiClO_4$), at different $[H^+]$ values: 2.0 (●), 1.5 (◆), 1.0 (▲), 0.75 (▼), and 0.50 (×)

spectra in 2.0 M $HClO_4$ are shown in Figure 1, with peaks λ/nm (ε/M^{-1} cm^{-1} per cube or trimer) at 236 (10 390), 503 (730), 603 (448), and 970 (122) for $[Mo_3FeS_4(H_2O)_{10}]^{4+}$, and 248 (8 219), 367 (5 550), and 602 (362) for $[Mo_3S_4(H_2O)_9]^{4+}$. These are in good agreement with previous values,[11,12] the former in 2M hpts (*p*-toluenesulphonic acid).

Solutions of O_2.—Air-saturated and (BOC cylinder) O_2-saturated 2 M $HClO_4$ aqueous solutions were used. Mixes of O_2 and N_2 of different ratios were also obtained from cylinder gases by adjustment of flow meters, and allowing two opposing gas streams to mix at a T-junction. Concentrations of O_2 were measured using a Beckmann oxygen analyser electrode (standardised against N_2-saturated and air-saturated water). The concentration of O_2 in air-saturated solutions was determined as 0.24 ± 0.01 mM, and in O_2-saturated solutions as 1.02 mM. Reactions were carried out in a 1-cm light-path spectrophotometer cell closed by a rubber septum. To eliminate air leaks in experiments with O_2 in excess (which required > 60 min) the same gas mix was passed through a glass vessel the size and shape of an inverted 15-cm^3 beaker positioned over the top of the spectrophotometer cell, which was fitted with a rubber septum. Gas entered *via* 2-mm tubing at the top of the vessel and escaped from around the base, which was in contact with a metal plate holding the spectrophotometer cell in place (partial seal was provided by 'Blue-tak' adhesive at this interface).

Stoicheiometry.—Absorbance changes were determined at 504 nm for the reaction of $[Mo_3FeS_4(H_2O)_{10}]^{4+}$ (0.20 mM) with O_2(0.010 mM) in 2.0 M $HClO_4$. The 1-cm spectrophotometer cell had N_2 over the solution. The O_2-containing solution was added by microsyringe. Mixing was achieved by moving a small bar magnet flea (≈4 mm long) inside the cell (without breaking the surface) using a bar magnet outside. With the cube in excess the ratio of $[Mo_3FeS_4(H_2O)_{10}]^{4+}$ consumed per mole of O_2 was 2.1 ± 0.1 : 1 from three determinations, and the stoicheiometry can therefore be expressed as in equation (1).

$$2Mo_3FeS_4^{4+} + O_2 + 4H^+ \longrightarrow 2Mo_3S_4^{4+} + 2Fe^{2+} + 2H_2O \quad (1)$$

Results

$[Mo_3FeS_4(H_2O)_{10}]^{4+}$ *in Excess.*—Runs were with $[O_2]$ in the range (0.07—0.30) × 10^{-4} M and $[Mo_3FeS_4(H_2O)_{10}{}^{4+}]$ (2.0—10.0) × 10^{-4} M. With O_2 in excess (see below) absorbance changes at 245 nm over the first ≈20 min provide evidence for the formation of intermediates. Here there may be similar less-intense changes at 245 nm within the first 4 min, followed by a uniphasic decrease in absorbance consistent with the conversion of $[Mo_3FeS_4(H_2O)_{10}]^{4+}$ into $[Mo_3S_4(H_2O)_9]^{4+}$. However, the trends are less clear because of the high background absorbance. Otherwise scan spectra indicate a retention of isosbestic points at 249, 286, 320, and 450 nm with < 1% changes over 3—4 half-lives. At 367 nm, which is an absorption peak for $[Mo_3S_4(H_2O)_9]^{4+}$, a uniphasic increase in absorbance (A) is observed, Figure 2. Plots of ln $(A_\infty - A_t)$ against time are linear for 3—4 half-lives, and give first-order rate constants $k_{obs.}$, Table. A linear dependence of $k_{obs.}$ on $[Mo_3FeS_4(H_2O)_{10}{}^{4+}]$ is obtained, Figure 3. Assuming formation of the intermediate $Mo_3FeS_4(O_2)^{4+}$ to be rate determining, the rate law is (2). On decreasing $[H^+]$ the rate constant k

Table. First-order rate constants $k_{obs.}$ (25 °C) for the reaction of $[Mo_3FeS_4(H_2O)_{10}]^{4+}$ (reactant in > 10-fold excess) with O_2 (1.5×10^{-5} M) determined from absorbance changes at 367 nm, I = 2.00 M ($LiClO_4$)

$[H^+]$/M	10^4 $[Mo_3FeS_4^{4+}]$/M	$10^4 k_{obs.}$/s^{-1}
2.0	10.0	19.3
	7.0	13.7
	5.5	10.5
	4.6	9.7[a]
	4.4	9.1[b]
	4.3	8.7[c]
	4.3	8.9[d]
	3.8	7.3
	2.0	3.7
1.5	10.0	15.9
	8.5	13.6
	7.1	11.1
	5.0	8.0
1.0	10.0	14.3
	8.0	11.6
	6.8	10.0
	5.4	7.8
	4.1	6.2
	3.5	5.0
0.75	9.0	11.9
	8.0	10.3
	7.0	8.3
	4.5	5.7
0.50	5.3	5.7
	4.7	4.9
	3.4	3.9
	2.0	2.0

[a] $[Fe(H_2O)_6^{2+}] = 5.1 \times 10^{-4}$ M added. [b] $[O_2] = 0.72 \times 10^{-5}$ M. [c] $[O_2] = 2.90 \times 10^{-5}$ M. [d] $[Mo_3S_4(H_2O)_9]^{4+} = 2.00 \times 10^{-4}$ M added.

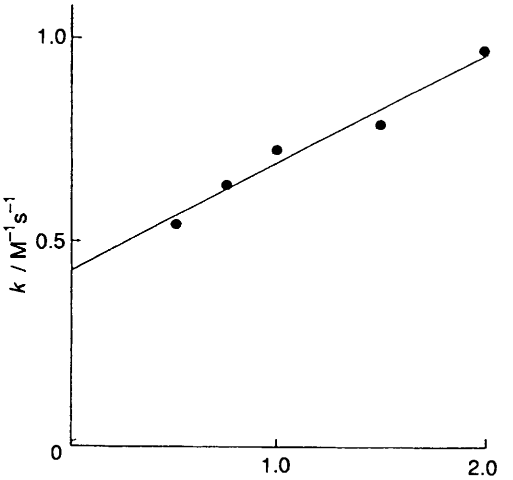

Figure 4. Dependence of second-order rate constant k (from the slopes in Figure 3) on $[H^+]$ at 25 °C, I = 2.00 M ($LiClO_4$)

$$d[Mo_3S_4^{4+}]/dt = 2k[Mo_3FeS_4^{4+}][O_2] \qquad (2)$$

$$k_{obs.} = 2k[Mo_3FeS_4^{4+}] \qquad (3)$$

decreases, Figure 4, and the dependence can be expressed as in (4). At 25 °C, I = 2.00 M ($LiClO_4$), $a = 0.43 \pm 0.03$ M^{-1} s^{-1} and $b = 0.26 \pm 0.02$ M^{-2} s^{-1}.

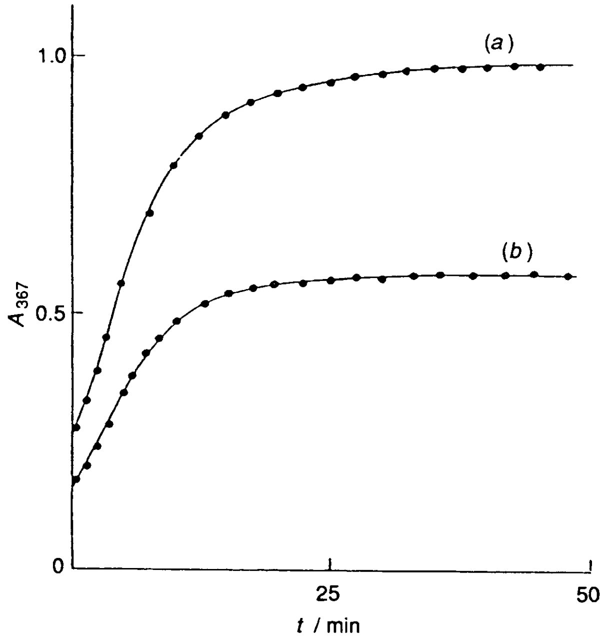

Figure 5. Absorbance changes (25 °C) at 367 nm with time for the reaction of O_2 (1.02 mM) with $[Mo_3FeS_4(H_2O)_{10}]^{4+}$ at 0.178 (*a*) and 0.104 mM (*b*), I = 2.00 M ($LiClO_4$)

$$k = a + b[H^+] \qquad (4)$$

O_2 *in Excess.*—At least two phases (the first effective over the first ≈5 min) were indicated from absorbance increases at 367 nm, Figure 5, $\Delta\varepsilon$ = 4 570 M^{-1} cm^{-1} for the overall conversion $[Mo_3FeS_4(H_2O)_{10}]^{4+} \longrightarrow [Mo_3S_4(H_2O)_9]^{4+}$. Similar observations were made at other wavelengths, *e.g.* 503 nm ($\Delta\varepsilon$ = 440 M^{-1} cm^{-1}, a decrease), Figure 1. Scan spectra, 230—260 nm, indicated a cross-over point which was not retained as an isosbestic, Figure 6. At a nearby wavelength of 245 nm ($\Delta\varepsilon$ = ≈200 M^{-1} cm^{-1}, a decrease) three phases are observed. Figure 7 illustrates the effect of varying $[Mo_3FeS_4(H_2O)_{10}^{4+}]$, and Figure 8 the effect of varying $[O_2]$. The slopes for the first and second phases exhibit approximate first-order dependences on $[Mo_3FeS_4(H_2O)_{10}^{4+}]$ (Figure 7) and $[O_2]$ (Figure 8). Since the involvement of two molecules of O_2 is unlikely, the first stage is assigned to (5), while in the second phase (5) (effective as a rapid prior equilibrium) is followed by (6). Thus from (5) and (6) the rate law (7) can be derived, and if $1 \gg K_1[O_2]$ a first-order dependence on each reactant follows for the second phase also.

$$Mo_3FeS_4^{4+} + O_2 \xrightleftharpoons{K_1} Mo_3FeS_4(O_2)^{4+} \qquad (5)$$

$$Mo_3FeS_4(O_2)^{4+} \xrightarrow{k_2} \text{products} \qquad (6)$$

$$\text{Rate} = \frac{K_1 k_2[Mo_3FeS_4^{4+}][O_2]}{1 + K_1[O_2]} \qquad (7)$$

For the third phase we note that A_∞ in Figures 7 and 8 varies relative to A_0. Varying amounts of $[Fe(H_2O)_6]^{3+}$ are formed, ε = 3 718 M^{-1} cm^{-1} at 245 nm in 2.0 M $HClO_4$, confirmed by addition of NCS^- when the red colour of $Fe(NCS)^{2+}$ is obtained. The formation of $[Fe(H_2O)_6]^{3+}$ and varying stoicheiometry make it difficult to apply a consecutive-reaction treatment in order to obtain rate constants. Such an approach requires well defined A_∞ values.[17,18] There are no similar signs

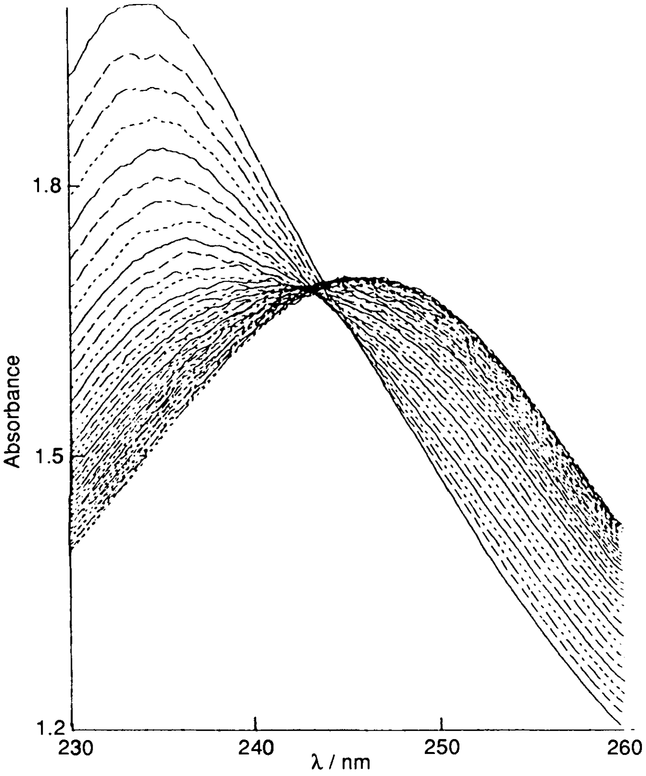

Figure 6. Scan spectra recorded at wavelength 230—260 nm for a run with $[Mo_3FeS_4(H_2O)_{10}]^{4+}$ at 0.20 mM and $[O_2]$ = 1.02 mM

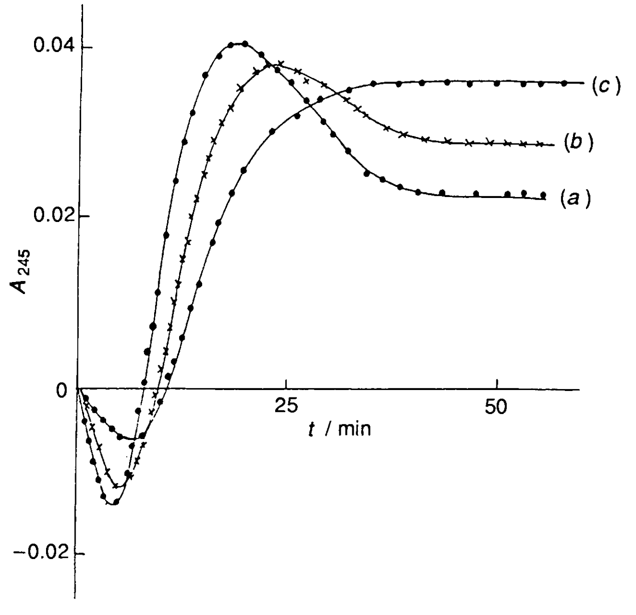

Figure 7. Absorbance (ΔA) *vs.* time changes for the reaction (25 °C) of O_2 (1.02 mM) with $[Mo_3FeS_4(H_2O)_{10}]^{4+}$ at 0.13 (*a*), 0.085 (*b*), and 0.050 mM (*c*) in 2.00 M $HClO_4$ at I = 2.00 M

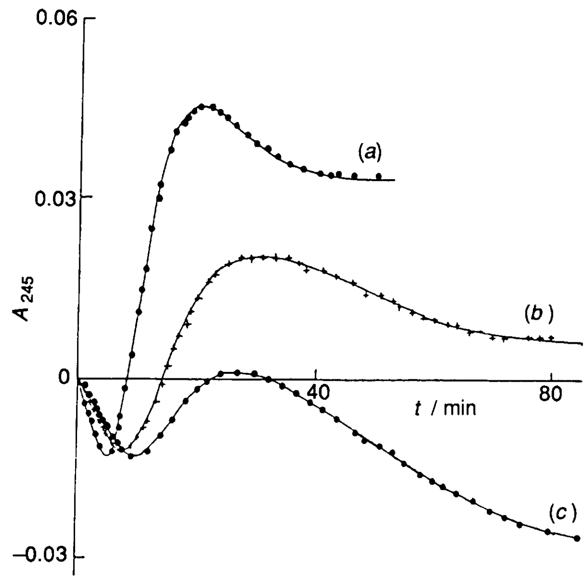

Figure 8. Absorbance (ΔA) *vs.* time changes for the reaction (25 °C) of $[Mo_3FeS_4(H_2O)_{10}]^{4+}$ (0.10 mM) with O_2 at 1.02 (*a*), 0.60 (*b*), and 0.47 mM (*c*) in 2.00 M $HClO_4$ at I = 2.00 M

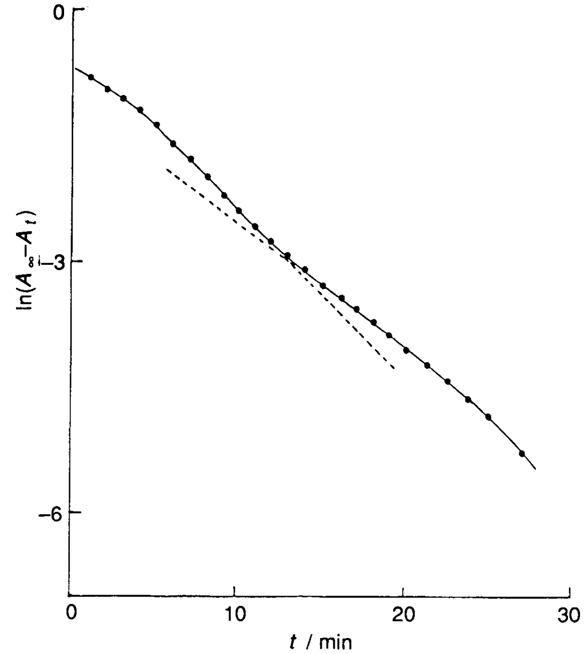

Figure 9. Typical first-order plot from absorbance changes at 367 nm for the reaction (25 °C) of $[Mo_3FeS_4(H_2O)_{10}]^{4+}$ (0.13 mM) with O_2 (1.02 mM) in 2 M $HClO_4$, I = 2.00 M. Absorbance changes over the first 5 min correspond to the first phase of reaction. The non-linearity of the remainder of the plot (defined as the second phase in *e.g.* Figure 5) suggests at least two processes as $Mo_3FeS_4(O_2)^{4+} \longrightarrow Mo_3S_4{}^{4+} + (FeO_2)$ with some contribution in the early stages from the fast reaction of $Mo_3FeS_4{}^{4+}$ with (FeO_2)

of $[Fe(H_2O)_6]^{3+}$ formation in runs with $[Mo_3FeS_4(H_2O)_{10}]^{4+}$ in excess, *e.g.* Figure 2.

Plots of $\ln(A_\infty - A_t)$ against time for runs at 367 nm, Figure 9, further indicate a complex reaction sequence. There was no single fit to the second phase, which gives rate constants in the range (2.4—3.4) × 10^{-3} s^{-1}. In the earlier stages of phase two there may be some reaction of $[Mo_3FeS_4(H_2O)_{10}]^{4+}$ with (FeO_2) (see below) even though the cube is not the reactant in excess.

Discussion

Substitution of only one H_2O by Cl^- on $[Mo_3FeS_4(H_2O)_{10}]^{4+}$ has been observed in a process which is too fast to monitor by stopped-flow spectrophotometry.[13] Since the rate constant is orders of magnitude faster than any substitution process yet determined for the Mo atoms of Mo_4 or Mo_3 clusters,[12,19,20] and intermediates are observed, it is likely that O_2 also substitutes at the Fe.

In cyclic voltammetry experiments described elsewhere[13] we were not able to generate $Mo_3FeS_4^{5+}$ and $Me_3FeS_4^{6+}$ forms, nor was any stable intermediate species observed in the reactions of $Mo_3FeS_4^{4+}$ with the one-equivalent oxidants $[Fe(H_2O)_6]^{3+}$ and $[Co(dipic)_2]^-$. It is unlikely therefore that the long-lived intermediates observed in this work have either of these formulae. The evidence obtained is consistent with a reaction scheme (8) and (9), where the bracketed iron(II) species

$$Mo_3FeS_4^{4+} + O_2 \longrightarrow Mo_3FeS_4(O_2)^{4+} \quad (8)$$

$$Mo_3FeS_4(O_2)^{4+} \longrightarrow Mo_3S_4^{4+} + (FeO_2) \quad (9)$$

liberated in phase two (runs with O_2 in excess), might be linear O_2H^- bonded as $Fe(O_2H)^+$, sideways bonded O_2^{2-} to give FeO_2, separated Fe^{2+} and H_2O_2 products, or a combination of these different possibilities. With $[Mo_3FeS_4(H_2O)_{10}]^{4+}$ in excess the relatively fast reaction (10) follows.

$$Mo_3FeS_4^{4+} + (FeO_2) + 4H^+ \longrightarrow Mo_3S_4^{4+} + 2Fe^{2+} + 2H_2O \quad (10)$$

The $[Mo_3FeS_4^{4+}]$ term in the rate law (2) arises from (8) and (9) and not the fast step (10). With O_2 in excess there may be some reaction (10) alongside the decomposition of (FeO_2), corresponding to Fe^{2+}/Fe^{3+}-catalysed decomposition of peroxide. A feature of the latter is that it yields $[Fe(H_2O)_6]^{3+}$ (which absorbs at 245 nm), the amount depending on the concentrations of reactants used. This makes a consecutive-reaction treatment difficult, and it has not, therefore, been possible to evaluate meaningful rate constants for runs with O_2 in excess. The second phase in Figures 7 and 8, corresponding to the major absorbance change at 367 nm, Figure 5, gives rate constants of the same magnitude as those from the major absorbance change in Figure 2. Since $[Mo_3FeS_4(H_2O)_{10}]^{4+}$ is itself a two-electron reductant, equation (11), formation

$$Mo_3FeS_4^{4+} - 2e^- \longrightarrow Mo_3S_4^{4+} + Fe^{2+} \quad (11)$$

of a long-lived μ-peroxo bi-cube intermediate, here written $Mo_3FeO_2FeMo_3^{8+}$, is not an obvious requirement to bring about the stepwise conversion $O_2 \longrightarrow O_2^{2-} \longrightarrow 2H_2O$. Such intermediates are a feature of reactions of O_2 with other metal-ion centres, in particular those of Co^{II},[3,4] but are also observed with the two-equivalent reductants Mo^{III} and V^{II}.[9,10] There is no evidence for a square dependence on the concentration of $[Mo_3FeS_4(H_2O)_{10}]^{4+}$, but this requirement is not an essential indicator. Thus a possible reaction sequence (12) and (13) would for example give only a first-order dependence

$$Mo_3Fe^{4+} + O_2 \xrightarrow{\text{slow}} Mo_3FeO_2^{4+} \quad (12)$$

$$Mo_3FeO_2^{4+} + Mo_3Fe^{4+} \xrightarrow{\text{fast}} Mo_3FeO_2FeMo_3 \quad (13)$$

on $[Mo_3FeS_4^{4+}]$. However, formation of a μ-peroxo di-cube is less likely to lead to the release of peroxide, and more likely to result in a direct conversion of O_2 into $2H_2O$. The formation of $[Fe(H_2O)_6]^{3+}$ in experiments with O_2 in large excess favours therefore a mechanism involving intermediate formation of $Mo_3FeO_2^{4+}$ only as the dominant process. Contributions from (13) cannot be excluded with $[Mo_3FeS_4(H_2O)_9]^{4+}$ the reactant in excess in which case the measured rate constant will correspond to the reaction step (12). The $[H^+]$-dependent term b in equation (4) is consistent with the tendency of O_2 to protonate as it is reduced to O_2^{2-} and then through to H_2O.

Because, with O_2 in excess, the third phase gives a net decrease in absorbance (Figures 7 and 8), it seems reasonable that an Fe^{2+}–O_2^{2-} adduct is released, and not Fe^{2+} and H_2O_2 which would be expected to give a smaller initial absorbance at 245 nm. Also on mixing equimolar amounts of Fe^{2+} and H_2O_2 (0.1 mM) the reaction monitored at 245 nm was found to be complete in $\approx$ 5 min. The longer time span (up to 50 min) for the third phase in Figures 7 and 8 is consistent with initial FeO_2 release. In one case (Figure 7) the absorbance changes for the second and third phases are superimposed due to the decrease in rate of the second phase. Amounts of $[Fe(H_2O)_6]^{3+}$ formed in the experiments with O_2 in excess were up to $\approx 30\%$ of total Fe. The Fe^{2+}/Fe^{3+}-catalysed decomposition of peroxide, with some $[Fe(H_2O)_6]^{3+}$ remaining on completion of the reaction, results in a stoicheiometry less than the 2:1 ratio indicated in (1). Reactions expected to conribute to the catalysed decomposition are as in (14)—(17). The chemistry here has been extensively studied.[21,22]

$$Fe^{2+} + H_2O_2 \longrightarrow Fe^{3+} + OH^- + OH^{\bullet} \quad (14)$$

$$Fe^{2+} + HO^{\bullet} \longrightarrow Fe^{3+} + OH^- \quad (15)$$

$$Fe^{3+} + H_2O_2 \longrightarrow Fe^{2+} + H^+ + HO_2 \quad (16)$$

$$Fe^{3+} + HO_2 \longrightarrow Fe^{2+} + H^+ + O_2 \quad (17)$$

To summarise, absorbance-time data for the $[Mo_3FeS_4(H_2O)_{10}]^{4+}$ reaction with O_2 can be accounted for qualitatively in terms of the formation of intermediates $Mo_3FeS_4(O_2)^{4+}$ and (FeO_2). Studies with $[Mo_3FeS_4(H_2O)_{10}]^{4+}$ in excess have yielded rate constants assigned to a composite term K_1k_2. In the latter there may be some contribution from a process involving formation of a $\mu(O_2^{2-})$ bi-cube intermediate.

Acknowledgements

P. W. D. thanks the S.E.R.C. for a research studentship.

References

1 L. E. Bennett, *Prog. Inorg. Chem.*, 1973, **18**, 1; O. Hayaishi (Editor), 'Molecular Mechanisms of Oxygen Activation,' Academic Press, New York, 1974; F. Basolo, B. M. Hoffman, and J. A. Ibers, *Acc. Chem. Res.*, 1976, **9**, 175; T. G. Spiro (Editor), 'Metal Ion Activation of Dioxygen,' Wiley, New York, 1980; A. G. Sykes, *Adv. Inorg. Bioinorg. Mech.*, 1982, **1**, 121; J. F. Endicott and K. Kumar, *ACS Symp. Ser.*, 1982, **198**, 425; E. C. Niederhoffer, J. H. Timmons, and A. E. Martell, *Chem. Rev.*, 1984, **84**, 137; 'Oxygen Complexes and Oxygen Activation by Transition Metals,' eds. A. E. Martell and D. T. Sawyer, Plenum, New York, 1988; H. Taube, *Prog. Inorg. Chem.*, 1986, **34**, 607.

2 (*a*) D. M. Stanbury, O. Hass, and H. Taube, *Inorg. Chem.*, 1980, **19**, 518; (*b*) I. I. Creaser, R. J. Geue, J. M. Harrowfield, A. J. Herlt, A. M. Sargeson, M. R. Snow, and J. Springborg, *J. Am. Chem. Soc.*, 1982, **104**, 6016; (*c*) A. Bakac, J. H. Espenson, I. I. Creaser, and A. M. Sargeson, *ibid.*, 1983, **105**, 7624.

3 S. Fallab and P. R. Mitchell, *Adv. Inorg. Bioinorg. Mech.*, 1984, **3**, 311.

4 A. G. Sykes and J. A. Weil, *Prog. Inorg. Chem.*, 1970, **13**, 1; R. G. Wilkins, *Adv. Chem. Ser.*, 1971, **100**, 111; G. McLendon and A. E. Martell, *Coord. Chem. Rev.*, 1976, **18**, 125.

5 R. M. Sellers and M. G. Simic, *J. Chem. Soc., Chem. Commun.*, 1975, 401; W. K. Wilmarth, H. Graff, and S. T. Gustin, *J. Am. Chem. Soc.*, 1956, **78**, 2683; M. Ardon and R. A. Plane, *ibid.*, 1959, **81**, 3197.

6 M. F. Tweedle and H. Taube, *Inorg. Chem.*, 1982, **21**, 3361.
7 P. George, *J. Chem. Soc.*, 1954, 4349; D-H. Chin, G. N. La Mar, and A. L. Balch, *J. Am. Chem. Soc.*, 1980, **112**, 4344.
8 J. S. Thompson, *J. Am. Chem. Soc.*, 1984, **106**, 4057; K. D. Karlin, Y. Gultneh, R. W. Cruse, J. C. Hayes, and J. Zubieta, *ibid.*, p. 3372. K. D. Karlin, R. W. Cruse, Y. Gultneh, A. Farooq, J. C. Hayes, and J. Zubieta, *ibid.*, 1987, **109**, 2668; Z. Tyeklar and K. D. Karlin, *Acc. Chem. Res.*, 1989, **22**, 241.
9 E. F. Hills, P. R. Norman, T. Ramasani, D. T. Richens, and A. G. Sykes, *J. Chem. Soc., Dalton Trans.*, 1986, 157.
10 J. D. Rush and B. H. Bielski, *Inorg. Chem.*, 1985, **24**, 4282.
11 T. Shibahara, H. Akashi, and H. Kuroya, *J. Am. Chem. Soc.*, 1986, **108**, 1342.
12 B-L. Ooi and A. G. Sykes, *Inorg. Chem.*, 1989, **28**, 3799.
13 P. W. Dimmock, D. P. E. Dickson, and A. G. Sykes, *Inorg. Chem.*, in the press.
14 T. Shibahara and H. Kuroya, *J. Coord. Chem.*, 1988, **18**, 233.
15 T. Shibahara, H. Akashi, and K. Hashinoto, *J. Inorg. Biochem.*, 1989, **36**, 178; International Conference Bioinorganic Chemistry, MIT, Boston, 1989, abstract to poster.
16 T. Shibahara, H. Akashi, and H. Kuroya, *J. Am. Chem. Soc.*, 1988, **110**, 3313.
17 A. A. Frost and R. G. Pearson, 'Kinetics and Mechanism,' 2nd edn., Wiley, New York, 1961, p. 160.
18 J. H. Espenson, 'Chemical Kinetics and Reaction Mechanism,' McGraw-Hill, New York, 1981, p. 65.
19 B-L. Ooi, C. Sharp, and A. G. Sykes, *J. Am. Chem. Soc.*, 1989, **111**, 125.
20 C. Sharp and A. G. Sykes, *J. Chem. Soc., Dalton Trans.*, 1988, 2579.
21 A. G. Sykes, 'Kinetics of Inorganic Reaction,' 2nd edn., Pergamon, Oxford, 1970, pp. 193—194.
22 N. Uri, *Chem. Rev.*, 1951, **50**, 375.

Received 3rd *April* 1990; *Paper* 0/01468K